G3: Genes|Genomes|Genetics Early Online, published on January 21, 2020 as doi:10.1534/g3.119.401023

The tempo and mode of angiosperm mitochondrial genome divergence inferred from intraspecific variation in *Arabidopsis thaliana*

Zhiqiang Wu*,†,1, Gus Waneka*,1, Daniel B. Sloan*,2

*Department of Biology, Colorado State University, Fort Collins, CO 80523
†Guangdong Laboratory of Lingnan Modern Agriculture, Genome Analysis Laboratory of the Ministry of Agriculture, Agricultural Genomics Institute at Shenzhen, Chinese Academy of Agricultural Sciences, Shenzhen, 518124, China.

1Authors contributed equally

2Corresponding author:
Daniel B. Sloan
1878 Campus Delivery
Fort Collins, CO 80523
dbsloan@rams.colostate.edu

Running Title: *Arabidopsis* mitogenome variation

Keywords: copy number variation, mutation accumulation line, mutation rate, recombination, single-nucleotide polymorphisms

ABSTRACT

The mechanisms of sequence divergence in angiosperm mitochondrial genomes have long been enigmatic. In particular, it is difficult to reconcile the rapid divergence of intergenic regions that can make non-coding sequences almost unrecognizable even among close relatives with the unusually high levels of sequence conservation found in genic regions. It has been hypothesized that different mutation/repair mechanisms act on genic and intergenic sequences or alternatively that mutational input is relatively constant but that selection has strikingly different effects on these respective regions. To test these alternative possibilities, we analyzed mtDNA divergence within *Arabidopsis thaliana*, including variants from the 1001 Genomes Project and changes accrued in published mutation accumulation (MA) lines. We found that base-substitution frequencies are relatively similar for intergenic regions and synonymous sites in coding regions, whereas indel and nonsynonymous substitutions rates are greatly depressed in coding regions, supporting a conventional model in which mutation/repair mechanisms are consistent throughout the genome but differentially filtered by selection. Most types of sequence and structural changes were undetectable in 10-generation MA lines, but we found significant shifts in relative copy number across mtDNA regions for lines grown under stressed vs. benign conditions. We confirmed quantitative variation in copy number across the *A. thaliana* mitogenome using both whole-genome sequencing and droplet digital PCR, further undermining the classic but oversimplified model of a circular angiosperm mtDNA structure. Our results suggest that copy number variation is one of the most fluid features of angiosperm mitochondrial genomes.

INTRODUCTION

The evolution of angiosperm mitochondrial genomes (mitogenomes) is a study in contrasts. On one hand, they exhibit exceptionally low nucleotide substitution rates, including at synonymous sites even though such sites are likely subject to relatively low levels of functional constraint (WOLFE *et al.* 1987; DROUIN *et al.* 2008). These low levels of sequence divergence are generally assumed to reflect unusually slow point mutation rates, especially when compared to high mitochondrial mutation rates in many other eukaryotic lineages (BROWN *et al.* 1979; SLOAN *et al.* 2017). However, direct measures of plant mitochondrial mutation rates are generally lacking, and the mechanisms that maintain such low levels of nucleotide substitutions are not known.

On the other hand, angiosperm mitogenomes are remarkably diverse at a structural level (MOWER *et al.* 2012b; GUALBERTO and NEWTON 2017). They are large and variable in size and subject to extensive rearrangements via recombination-mediated mechanisms, which may be accelerated under conditions of plant stress (ARRIETA-MONTIEL and MACKENZIE 2011). Although they typically map as circular structures, their actual physical form appears to be far more complex and variable (BENDICH 1993; SLOAN 2013; KOZIK *et al.* 2019).

Comparisons among angiosperm mitochondrial genomes often find that large fractions of intergenic sequence are unalignable between species and seemingly unique to individual lineages (KUBO and NEWTON 2008). In the most extreme cases, only about half of intergenic sequence content may be shared even between two different mitochondrial haplotypes from the same species (SLOAN *et al.* 2012). There are likely at least two mechanisms responsible for this phenomenon. First, angiosperm mitogenomes are frequent recipients of large quantities of horizontally transferred DNA from the plastid genome, nucleus, and other sources (ELLIS 1982; GOREMYKIN *et al.* 2012; RICE *et al.* 2013). As such, many intergenic sequences are recently acquired and truly lack homologous sequences in mitogenomes of other angiosperms. It is unlikely, however, that horizontal transfer can provide a full explanation because a lot of intergenic content cannot be traced to any potential donor source. A second possible mechanism is that rates of sequence and structural evolution are so fast in the intergenic regions of angiosperm mitogenomes that homologous sequences can become essentially unrecognizable even among closely related species. But this latter explanation presents a paradox when juxtaposed with the observation that genic regions in plant mitogenomes can exhibit some of the slowest known rates of nucleotide substitutions.

Christensen (2013; 2014) has proposed alternative models to explain the striking contrast in evolutionary rates between genic and intergenic regions in angiosperm mitogenomes, which are based either on differences in mutational input or differences in selection between these two types of regions. Under the mutational-input model, the contrasting rates of divergence would reflect systematic differences between genic and intergenic sequences with respect to DNA polymerase

errors during replication, exposure to DNA damage, and/or the efficacy of DNA repair processes. It was hypothesized that transcription-coupled repair (HANAWALT and SPIVAK 2008) could have such an effect in altering mutation rates in expressed vs. non-expressed regions in angiosperm mitogenomes (CHRISTENSEN 2013), but subsequent analysis of substitution rates in transcribed non-coding regions did not find support for this hypothesis (CHRISTENSEN 2014). Nevertheless, the possibility of systematic differences in mutational input among regions within plant mitochondrial genomes remains largely untested, and it has been observed that some species can exhibit substantial rate variation even from one gene to the next for reasons that remain unclear (ZHU *et al.* 2014; WARREN *et al.* 2016).

An alternative and perhaps more conventional model is that mutational input is relatively consistent across the genome but that genic vs. intergenic regions are subject to very different selection pressures. For example, structural and sequence variation introduced by error prone repair pathways may be filtered out in gene regions but largely neutral and tolerated in non-coding regions (CHRISTENSEN 2014). This may be especially true for any repair mechanisms that lead to structural rearrangements or indels that would truncate protein-coding genes. One prediction from this model is that rates of single-nucleotide substitutions in intergenic regions should largely match those at relatively neutral sites in protein-coding sequences (e.g., synonymous sites). However, this prediction has been difficult to test because finding sets of genomes that have enough divergence in coding regions to estimate substitution rates and still retain enough similarity in intergenic structure and content to align these non-coding regions is a challenge.

In this sense, variation at an intraspecific scale may be informative, as comparisons between patterns of recent and long-term evolutionary change can be powerful in separating effects of mutation and selection (NIELSEN 2005). A previous pairwise comparison between two different *Arabidopsis thaliana* accessions was used to measure mitochondrial sequence divergence, but this analysis only identified a single synonymous nucleotide substitution in protein-coding genes and thus could offer little precision in quantifying the frequency of single nucleotide polymorphisms (SNPs) in different functional sequence categories (CHRISTENSEN 2014). The study was further complicated by the large number of sequencing errors that were later identified in the early *A. thaliana* mitogenome reference sequences (SLOAN *et al.* 2018).

Here, we take advantage of the ever-growing amount of genomic resources in *A. thaliana*, including the sequencing of complete genomes from the 1001 Genomes Project (ALONSO-BLANCO *et al.* 2016) and from mutation accumulation (MA) lines in this species (JIANG *et al.* 2014), to generate more robust polymorphism datasets for investigating the mechanisms of mitogenome divergence. Our goal is to distinguish among alternative explanations for the contrasting rates of genic vs. intergenic sequence evolution and identify the genomic changes that accrue most rapidly during angiosperm mitogenome evolution.

MATERIALS AND METHODS

Identification of intraspecific mitogenome variation from the *Arabidopsis* 1001 Genomes Project

To analyze standing mitochondrial polymorphisms within *A. thaliana*, raw Illumina reads from the 1001 Genomes Project (which actually contains 1135 sequenced individuals; ALONSO-BLANCO *et al.* 2016) were downloaded from the NCBI Sequence Read Archive (SRA) under the project accession SRP056687 using the fastq-dump tool in the NCBI SRA Toolkit v2.9.6. For larger datasets, only the first 20 million read pairs were downloaded. Illumina adapter sequences were trimmed with Cutadapt v2.1 (MARTIN 2011), applying a q20 quality cutoff, a 15% error rate for matching adapter sequences, and a minimum trimmed read length of 50 bp. As such, 88 of the 1135 sequenced individuals were excluded entirely from the analysis because their original read lengths were shorter than 50 bp. Trimmed reads were mapped to the *A. thaliana* Col-0 GenBank RefSeq accessions for the mitochondrial (NC_037304.1) and plastid genomes (NC_000932.1) using Bowtie v2.3.5 (LANGMEAD and SALZBERG 2012). By competitively mapping sequence reads against both organelle genomes, we avoided erroneously mapping plastid-derived reads to related regions in the mitogenome resulting from historical plastid-to-mitochondrial DNA transfers (i.e., *mtpts*; ELLIS 1982; SLOAN and WU 2014). The resulting alignment files were sorted with SAMtools v1.9 (LI *et al.* 2009), and variants were called using the HaplotypeCaller tool in GATK v4.1.0.0 (MCKENNA *et al.* 2010) with ploidy level set to 1 after removing duplicate reads with the GATK MarkDuplicates tool. Coverage depth at each position in the mitogenome was calculated with the SAMtools depth function. The resulting variant sets were filtered to require a minimum site-specific coverage depth of 50. Variants were also excluded if their coverage was less than half or more than three times the median genome-wide coverage. These thresholds were applied to avoid erroneously identifying variants based on low-frequency sequences such as nuclear insertions (i.e., *numts*; STUPAR *et al.* 2001; HAZKANI-COVO *et al.* 2010) or based on mis-mapping to repeats within the genome.

To distinguish between ancestral and derived alleles that are segregating within *A. thaliana*, we aligned the *A. thaliana* reference genome against the *Brassica napus* mitogenome (NC_008285.1), using NCBI BLASTN v2.2.30+, applying a minimum alignment length of 400 bp and a minimum nucleotide identity of 90%. The *B. napus* allele for all alignable *A. thaliana* SNP positions was extracted from the BLAST output with a custom BioPerl script (STAJICH *et al.* 2002), which is available via GitHub (https://github.com/dbsloan/polymorphism_athal_mtdna). An alternative approach to distinguish between ancestral and derived alleles is based on the fact that derived alleles are typically at low frequency. As such, even when it is not possible to polarize a variant with

130 an outgroup because it is found in an unalignable region, reasonable predictions of ancestral vs.
131 derived state can still be based on current allele frequencies. Therefore, we calculated allele
132 frequencies at each variable site to identify the minor allele, using all samples within the 1001
133 Genomes Project that met our coverage requirements for variant calling (see above).
134 Positions within the *A. thaliana* reference mitogenome were partitioned into functional
135 categories (protein-coding, rRNA, tRNA, introns, pseudogenes, and intergenic) based on the RefSeq
136 annotation (NC_037304.1). PAML v4.9a was used to approximate the total number of synonymous
137 and nonsynonymous 'sites' within protein-coding sequence (accounting for the partial degeneracy at
138 some positions owing to two- and three-member codon families).
139
140 **Analysis of mitogenome divergence in *Arabidopsis* mutation accumulation lines**
141 To analyze short-term divergence in *A. thaliana* mitogenomes, we obtained raw Illumina reads from
142 the MA lines generated by Jiang et al. (2014) from NCBI SRA (SRP045804). MA lines involve
143 bottlenecking each generation through single-seed descent to limit selection on organismal fitness
144 and obtain a relatively unfiltered view of *de novo* mutation accumulation (HALLIGAN and KEIGHTLEY
145 2009). This dataset consisted of a total of six MA lines, each propagated for 10 generations. Three
146 lines were propagated under benign growing conditions, while the other three were subjected to salt
147 stress each generation, except in the final generation in which all lines were grown under the same
148 benign conditions. Three biological replicates from each of the six lines were sequenced in the
149 original study (JIANG *et al.* 2014).
150 To test for *de novo* nucleotide substitutions and indels in the mitogenomes of these MA lines,
151 we applied the same variant calling pipeline as described above for the 1001 Genomes samples.
152 The only modification was that we set the ploidy level to 10 so that we could potentially detect any
153 novel variants that were heteroplasmic at a frequency of ~10% or greater. There are many causes
154 that can lead to erroneous identification of *de novo* mitochondrial variants, including mapping
155 artefacts, *numts*, and heteroplasmies inherited from the original parent. To avoid such errors, we
156 focused on variants that were unique to one or more replicates from a single MA line. For all such
157 variants predicted by our pipeline, we manually inspected read alignments using IGV (ROBINSON *et*
158 *al.* 2017) to determine whether they were detectable in samples from other MA lines.
159 We analyzed copy number variation across the *A. thaliana* mitogenome by normalizing site-
160 specific data for depth of sequence coverage as counts per million mapped read (CPMM) values
161 and averaging them into non-overlapping windows of 500 bp. To avoid any effects of cross-mapping
162 from plastid-derived reads, which are highly abundant in total-cellular DNA samples, we excluded
163 any windows that overlapped with previously identified *mtpts* (SLOAN and WU 2014). We also
164 excluded the first and last windows because of potential bias in mapping at the edges where the
165 circular mitogenome map was arbitrarily cut into a linear sequence. To try to account for coverage

166 bias introduced during the sequencing process because of differences in local nucleotide
167 composition (AIRD *et al.* 2011; VAN DIJK *et al.* 2014), we fit these data to a linear model that included
168 GC content and a count of homopolymers of greater than 7 bp in length as independent variables to
169 predict CPMM in each window. This model was implemented in R v3.6.0 using the lm function. The
170 subsequent analyses of copy number variation described below were performed with both the raw
171 CPMM values and the residuals from this model.
172 To test for associations in coverage values between adjacent windows across the
173 mitogenome, we performed a Wald–Wolfowitz runs test, using the runs.test function in the R
174 randtests package. To test for significant divergence in coverage values among the MA lines, we fit
175 a model with treatment (salt-stressed vs. control) as a fixed effect and MA line as a nested random
176 effect. This test was implemented in R with the lmer function and the lme4 and lmerTest R
177 packages. We controlled for multiple comparisons by applying a false discovery rate (FDR)
178 correction (BENJAMINI and HOCHBERG 1995).
179 We also examined the frequency of alternative genome conformations associated with
180 recombination between small repeats by first mapping Illumina reads to the *A. thaliana* Col-0
181 reference mitogenome with BWA v0.7.12, using the mem command and the -U 0 option. We then
182 used a custom Perl script (https://github.com/dbsloan/polymorphism_athal_mtdna) to parse the
183 resulting alignment file. For each pair of repeats in the mitogenome, this script calculated the number
184 of read pairs that mapped in a concordant fashion spanning a repeat as well as the number of read
185 pairs that mapped discordantly but in locations that were consistent with a recombination event
186 between the pair of repeats. This analysis was performed on all repeat pairs between 100 and 500
187 bp in length with a minimum of 80% nucleotide sequence identity. We then tested whether the
188 frequency of recombinant conformations for each repeat pair differed significantly among MA lines
189 by once again fitting a model with treatment as a fixed effect and MA line as a nested random effect
190 (see coverage analysis described above).
191
192 **Mitochondrial DNA purification and Illumina sequencing**
193 Three full-sib families from our *A. thaliana* Col-0 lab stock were grown in a growth chamber under
194 short-day conditions (10 h of light at 100 μmole m^{-2} s^{-1}) at 23 °C. For each family, 30-40g of rosette
195 tissue was harvested from plants after 6-7 weeks of growth. To reduce starch content, plants were
196 kept in the dark for two days prior to collecting leaf tissue, and then the harvested tissue was stored
197 overnight in the dark at a 4 °C. All subsequent tissue-processing and DNA-extraction steps were
198 carried out in a 4 °C cold room or refrigerated centrifuge unless stated otherwise.
199 Leaf tissue was disrupted in high salt isolation buffer (1.25 M NaCl, 50 mM Tris-HCl pH 8.0,
200 5 mM EDTA, 0.5% polyvinylpyrrolidone, 0.2% bovine serum albumin, 15 mM β-mercaptoethanol),

201 using 10 ml of buffer per g of tissue. Disruption was performed with a standard kitchen blender and a
202 series of five bursts of ~10 s each with ~10 s of settling time between each burst, followed by
203 filtration through four layers of cheesecloth and one layer of Miracloth. Filtrates were then
204 centrifuged at 150 rcf for 15 min. The resulting supernatant was transferred to new bottles and
205 centrifuged at 1500 rcf for 20 min. The supernatant was then again transferred to new bottles and
206 centrifuged at 15,000 rcf for 20 min. After discarding the resulting supernatant, the mitochondrial
207 pellets, were gently but thoroughly resuspended in 3 ml of DNase buffer (0.35 M sorbitol, 50 mM
208 Tris-HCl pH 8.0, 15 mM $MgCl_2$) with a paintbrush. Then 7 ml of DNase solution (DNase I dissolved in
209 DNase buffer at a concentration of 1 mg/ml) was added to each resuspended pellet. The samples
210 were incubated on ice for 1 h with occasional gentle swirling to digest contaminating plastid and
211 nuclear DNA. Three volumes of wash buffer (0.35 M sorbitol, 50 mM Tris-HCl pH 8.0, 25 mM EDTA)
212 was added to each sample followed by centrifugation at 12,000 rcf for 20 min. The resulting pellets
213 were washed two more times by resuspending in 20 ml wash buffer and centrifuging at 12,000 rcf for
214 20 min. The final washed pellet was resuspended in 1 ml wash buffer. One-twentieth volume of a 20
215 mg/ml proteinase K solution was added and incubated at room temperature for 30 min. Mitochondria
216 were lysed by adding one-fifth volume of lysis buffer (5% N-lauryl sarcosine Na salt; 50 mM Tris-HCl
217 pH 8.0, 25 mM EDTA) followed by gentle mixing by inversion for 10 min at room temperature. One
218 volume of phenol:chloroform:isoamyl alcohol (25:24:1) was added followed by vortexing for 5 s and
219 centrifugation at 12,000 rcf for 10 min. The resulting aqueous phase was transferred to a new tube
220 and incubated with 4 µl of a 10 mg/ml RNase A solution. The samples were then treated with two
221 rounds of cleanup with phenol:chloroform:isoamyl alcohol as described above followed by
222 precipitation with one volume of ice-cold isopropanol and incubation for at least 20 min at -20 °C.
223 Precipitated DNA was pelleted by centrifugation at 12,000 rcf for 10 min and washed twice with 500
224 µl of ice-cold 70% ethanol. The final DNA pellet was air dried and dissolved in TE buffer (10 mM
225 Tris-HCl pH 8.0, 1 mM EDTA).
226 Sequencing libraries were produced for each of the three resulting mtDNA samples, using
227 the NEBNext Ultra II FS DNA Library Prep Kit. We used 50 ng of input DNA, with a 15 min
228 fragmentation step, and 5 cycles of PCR amplification. The resulting libraries had an average insert
229 size of approximately 245 bp and were sequenced on a NovaSeq 6000 platform (2×150 bp),
230 producing between 14.1M and 15.4M read pairs per library. The reads were used for coverage-
231 depth analysis by mapping to the *A. thaliana* reference mitogenome as described above for the MA-
232 line dataset.
233
234 **ddPCR copy number analysis**

235 To confirm variation in copy number that was inferred from deep sequencing data across the
236 mitogenome, we performed droplet digital PCR (ddPCR). Primers were designed to target six
237 regions with high sequencing coverage and six regions with low coverage (Table S1). Analysis, was
238 performed on the same three purified mtDNA samples described above and one sample of total-
239 cellular DNA extracted from the same *A. thaliana* Col-0 lab line, using a modified CTAB and
240 phenol:chloroform protocol (DOYLE and DOYLE 1987). The template quantity for each reaction was
241 either 2 pg of mtDNA or 400 pg of total-cellular DNA, with two technical replicates for each reaction.
242 All ddPCR amplifications were set up in 20-µL volumes with Bio-Rad QX200 ddPCR EvaGreen
243 Supermix and a 2 µM concentration of each primer before mixing into an oil emulsion with a Bio-Rad
244 QX200 Droplet Generator. Amplification was performed on a Bio-Rad C1000 Touch Thermal Cycler
245 with an initial 5 min incubation at 95 °C and 40 cycles of 30 s at 95 °C and 1 min at 60 °C, followed
246 by signal stabilization via 5 min at 4 °C and 5 min at 95 °C. The resulting droplets were read on a
247 Bio-Rad QX200 Droplet Reader. Copy numbers for each PCR target were calculated based on a
248 Poisson distribution using the Bio-Rad QuantaSoft package. To assess significant difference in
249 copy-number between the sets of primers from high- and low-coverage regions of the mitogenome,
250 one-tailed t-tests were performed for each of the four DNA samples, using the means for each pair
251 of technical replicates as input.
252
253 **Data Availability**
254 All newly generated and previously published sequence data are available via NCBI SRA. Newly
255 generated Illumina data were deposited under accession PRJNA546277. Custom scripts used in
256 data analysis are available via GitHub (https://github.com/dbsloan/polymorphism_athal_mtdna).
257 Data pertaining to identified sequence variants and copy-number variation are provided in
258 supplementary Figures S1-S4 and Tables S1-S4 submitted via https://gsajournals.figshare.com.
259
260
261 **RESULTS**
262
263 **Intraspecific mitochondrial sequence variation in the *Arabidopsis thaliana* 1001 Genomes**
264 **Project**
265 Using whole-genome resequencing data from the 1001 Genomes Project, we identified a total of
266 1105 mitochondrial SNPs that are variable across *A. thaliana* accessions, including three sites at
267 which three different alleles were detected (Table S2). For a subset of 319 of these sites, we could
268 infer the ancestral state by aligning the nucleotide position to the outgroup *Brassica napus*. We could
269 also infer the polarity of changes for the entirety of the dataset by assuming that the minor allele
270 represented the derived state. This allele-frequency method produced the same call for 87% of the

271 319 *Brassica*-polarized SNPs, suggesting that it had substantial predictive value. Both of these
272 approaches revealed a mutation spectrum that is heavily biased towards increasing AT content.
273 Substitutions that increased AT content were 7-fold more common than those that decreased it
274 based on the *Brassica*-polarized dataset and 5-fold more common in the full dataset based on allele
275 frequency (Table S2). The spectrum did not exhibit the large overrepresentation of transitions that is
276 found in mtDNA of some eukaryotes (YANG and YODER 1999), with an overall transition:transversion
277 ratio of 422:686 that was only modestly above the null expectation of 1:2 (Table S2). However,
278 AT→TA and GC→CG transversions were rare, representing only 7% and 10% of all transversions,
279 respectively (Table S2). This mutation spectrum is generally consistent with observations from a
280 published pairwise comparison between the *A. thaliana* Col-0 and C24 ecotypes (CHRISTENSEN
281 2013). The extreme AT bias is also consistent with a previous analysis of inserted plastid sequences
282 (*mtpts*) as relatively neutral markers in angiosperm mtDNA (SLOAN and WU 2014). Although that
283 study found that angiosperm mitogenomes generally had weak AT bias, it identified *A. thaliana* as an
284 outlier with a much stronger bias than most species. Therefore, the inferred mitochondrial mutation
285 spectrum from *A. thaliana* may not be broadly representative of angiosperms with respect to AT
286 bias.
287 By comparing the distribution of SNPs across different functional classes within the
288 mitogenome, we found that the presence of base-substitutions is 2.9-fold lower in protein-coding and
289 RNA genes than in intergenic regions (Table 1). However, if only synonymous SNPs in protein-
290 coding genes are considered, the SNP abundance is much more similar but remains slightly lower in
291 genes (0.0027 per synonymous site) than in intergenic regions (0.0034 per site). The average minor
292 allele frequency was also slightly lower for synonymous SNPs (0.016) than for SNPs in intergenic
293 regions (0.026).
294 In contrast to the relatively similar SNP levels between synonymous sites and intergenic
295 regions, there was a radical difference in the distribution of indels across functional classes in the *A.*
296 *thaliana* mitogenome. A total of 190 polymorphic indels were identified in the 1001 Genomes
297 dataset, and every one of them was located in either an intergenic region or an intron (Table 1).
298 Overall, within gene sequences, we found a large reduction of variants that are expected to be
299 disruptive of gene function (i.e., nonsynonymous substitutions and indels) but limited evidence of
300 reduced abundance of changes that are likely to be relatively neutral (i.e., synonymous
301 substitutions).
302
303 **Shifts in mitochondrial copy-number variation across mutation accumulation lines**
304 By analyzing mitochondrial reads from published whole-genome resequencing data of *A. thaliana*
305 MA lines (JIANG *et al.* 2014), we found that most potential mitogenome changes were undetectable
306 over a timescale of 10 generations, regardless of whether the lines had been propagated under salt-

307 stressed or benign conditions. We did not detect any SNPs or indels that reached homoplasmy in
308 individual lines. Our pipeline identified a total of 11 low-frequency variants (seven SNPs, two indels,
309 and two multinucleotide variants with multiple changes clustered at nearby sites) that were unique to
310 a single MA line and thus candidates for *de novo* mutations. However, manual inspection of read
311 alignments found evidence of these same variants at low frequencies in other lines, indicating that
312 they were unlikely to be true *de novo* mutations. Therefore, we did not find any convincing evidence
313 of novel substitutions or small indels present in the heteroplasmic state. Angiosperm mitogenomes
314 are known to undergo frequent, homogenizing recombination between large repeat sequences and
315 lower frequency recombination between short repeat sequences (<500 bp), which can lead to shifts
316 in the relative frequency of alternative structures (SMALL *et al.* 1987; LONSDALE *et al.* 1988; ARRIETA-
317 MONTIEL *et al.* 2009; GUALBERTO and NEWTON 2017). To test for such structural changes, we
318 quantified the frequency of recombinant conformations using read-pairs spanning short repeat
319 sequences. Although we identified minor variation in frequencies of alternative conformation across
320 sequenced lines (Table S3), none of these showed consistent patterns of divergence for either
321 treatment or line effects at an FDR of 0.05.
322 In mapping MA line reads to the *A. thaliana* reference mitogenome, we observed variation in
323 coverage across the length of the genome, which was broadly similar in the six different MA lines
324 (Figure 1). Because Illumina DNA sequencing (and the PCR-based techniques it relies on) can be
325 biased against sequences with extreme GC or AT richness or with low-complexity features like
326 homopolymers (AIRD *et al.* 2011; VAN DIJK *et al.* 2014), it is possible that the observed coverage
327 variation was an artefact of amplification/sequencing bias. To investigate this possibility, we fit a
328 model to predict sequencing depth based on GC content and presence of homopolymers. This effort
329 was only able to explain a low percentage of the variance in sequencing depth across the
330 mitogenome (R^2 < 0.3 for all datasets), and the general pattern of copy number variation was
331 retained after controlling for this effect (Figure S1), suggesting that bias associated with simple
332 nucleotide-composition features was not the primary cause of the observed variation. For
333 subsequent analyses of coverage depths, we also used the residuals from these models to account
334 for sequencing bias related to nucleotide composition.
335 To assess whether there were any significant shifts in copy-number variation during
336 propagation of MA lines, we scanned the length of the genome in 500-bp windows to test for effects
337 at the level of treatment (salt-stressed vs. control) and individual MA lines. We found that many of
338 the 713 windows in the mitogenome showed small but significant differences between treatments
339 after an FDR correction for multiple comparisons (35 windows when using raw CPMM values and 14
340 when using residuals from a nucleotide composition model; Figures 2 and S2; Table S4). None of
341 the windows were significant for an MA-line effect after the same FDR correction, where line was
342 tested as a nested effect within treatment (Table S4). Adjacent regions tended to show coverage

343 differences in the same direction relative to the genome-wide median (Wald–Wolfowitz runs test;
344 only 201 observed cases in which adjacent windows were on opposite sides of the median
345 compared to a null expectation of 356; $P << 0.001$). Therefore, we found evidence that MA lines
346 shifted in consistent ways with respect to region-specific copy number when subjected to stressed
347 vs. benign growing conditions over 10 generations. Although the effect sizes were modest (up to a
348 20.5% shift in coverage in stressed vs. control samples), they could still be detected with a relatively
349 small sample size because of the consistent patterns across replicate lines.
350
351 **Sequencing and ddPCR analysis of purified *Arabidopsis thaliana* mtDNA**
352 To further test for evidence of copy number variation within the *A. thaliana* mitogenome, we purified
353 mtDNA from replicate families of our own lab line of the Col-0 ecotype. Illumina sequencing of these
354 samples resulted in 67-68% of reads mapping to the *A. thaliana* reference mitogenome for each
355 biological replicate, demonstrating substantial enrichment for mtDNA. An additional 6-8% and 1-3%
356 of reads could be mapped to the *A. thaliana* plastid and nuclear genomes, indicating some
357 contamination from other genomic compartments. The remaining unmapped reads were dominated
358 by known plant-associated bacteria (e.g., *Pseudomonas* and *Enterobacter*), which appear to have
359 been co-enriched in our mitochondrial isolations. As found with the MA lines, this analysis revealed a
360 heterogeneous pattern of coverage across the mitogenome, which was generally consistent among
361 the three replicates (Figures 3 and S3). Once again, we found that adjacent regions tended to show
362 coverage variation in the same direction (Wald–Wolfowitz runs test; only 120 observed cases in
363 which adjacent windows were on opposite sides of the median compared to a null expectation of
364 356; $P << 0.001$). However, comparing between our samples and the MA lines found only a modest
365 correlation in copy number variation ($r < 0.25$; Figure S4).
366 To confirm that the observed heterogeneity in coverage was a product of true variation in
367 copy number rather than an artefact of sequencing bias, we performed ddPCR with two sets of six
368 markers that were selected for either high-coverage or low-coverage regions based on sequencing
369 data (Figure 3). Unlike sequencing and traditional qPCR, this method is generally insensitive to
370 variation in PCR efficiency or amplification bias because it is based on endpoint PCR (40 cycles)
371 within each 'micro-reactor' droplet. We found significant differences in copy number between the
372 sets of high- and low-coverage markers for both the purified mtDNA samples that were used in
373 sequencing and a total-cellular DNA extraction ($P < 0.001$ for each of the three purified mtDNA
374 samples and $P = 0.011$ for the total-cellular DNA sample; Figure 4). In all cases, the average
375 difference in copy number between these sets was somewhat smaller (between 17.1% and 20.3%
376 for the purified mtDNA samples and 10.7% for the total-cellular sample) than from sequence
377 estimates (mean of 36.3%), which may reflect some regression to the mean because the high- and

378 low-copy markers were chosen only based on being in the extreme tails of the sequencing-coverage
379 distribution rather than for an *a priori* reason.
380
381
382 **DISCUSSION**
383
384 **Contrasting rates of evolution in genic and intergenic regions of angiosperm mitogenomes**
385 Our analysis confirmed dramatic differences in rates of mitogenome structural evolution between
386 genic and intergenic regions at an intraspecific level within *A. thaliana*, mirroring the extensive
387 observations of this phenomenon based on divergence between angiosperm species (KUBO and
388 NEWTON 2008). By dramatically expanding the number of sampled accessions with the aid of the
389 1001 Genomes dataset (ALONSO-BLANCO *et al.* 2016), we were also able to make quantitative
390 comparisons between nucleotide substitution rates in these regions, which was previously difficult
391 because of the limited number of substitutions in an earlier comparison between two *A. thaliana*
392 accessions (CHRISTENSEN 2013). The similar levels of nucleotide substitutions between intergenic
393 regions and synonymous sites in protein-coding genes (Table 1) suggests that mutational input in
394 different functional regions is comparable. As such, the most likely explanation for the divergent
395 evolutionary rates in genic and intergenic regions is a conventional model, under which selection has
396 varying effects in filtering mutations in different region throughout the genome (CHRISTENSEN 2014).
397 Despite the rough similarity between nucleotide substitution rates at synonymous sites and in
398 intergenic regions, we still found that the synonymous rate was slightly lower (Table 1). There are
399 multiple possible explanations for this gap. First, it is possible synonymous substitution rates are
400 suppressed because these sites still experience a larger degree of purifying selection than intergenic
401 regions. For example, even if they do not change amino acid sequences, synonymous substitutions
402 can disrupt the translation efficiency, secondary structure, or binding motifs of mRNAs (CHAMARY *et*
403 *al.* 2006). Indeed, there is evidence for some weak purifying selection acting on synonymous sites in
404 angiosperm mitogenomes (SLOAN and TAYLOR 2010; WYNN and CHRISTENSEN 2015). Selection on
405 multinucleotide mutations may also affect observed synonymous substitution rates. There is a
406 growing appreciation that clustered substitutions at adjacent sites can occur in a single mutational
407 event (SCHRIDER *et al.* 2011; HARRIS and NIELSEN 2014) and that they can affect inferences of
408 selection (VENKAT *et al.* 2018). It is very likely that some of the SNPs observed at adjacent sites in
409 our analysis (Table S1) do not represent independent events. When such events occur in protein-
410 coding genes, synonymous mutations may be removed by selection because they are linked to
411 harmful mutations at adjacent nonsynonymous sites, whereas multinucleotide mutations in
412 intergenic regions may remain relatively neutral. There are also mechanisms that may inflate
413 substitution rate estimates in intergenic regions. For example, these regions often contain short,

414 non-identical repeats that can undergo rare recombination events and create rearrangements
415 (ARRIETA-MONTIEL *et al.* 2009; GUALBERTO and NEWTON 2017). Such recombination events can give
416 the false impression that conventional nucleotide substitutions occurred because they create
417 chimeric versions of similar but non-identical sequences.
418 Regardless of the causes of the small observed gap between substitution rates at
419 synonymous sites vs. intergenic regions, it is clear that the magnitude of this difference is trivial
420 relative to the wildly different rates of overall divergence observed between genes and the rest of the
421 mitogenome in angiosperms. Indeed, it may simply reflect sampling variance as the small difference
422 between intergenic regions and synonymous sites (0.0034 vs. 0.0027) is not even statistically
423 significant ($\chi^2 = 0.8$; $P = 0.37$). While it is possible that certain mutational mechanisms preferentially
424 act in intergenic regions and make them mutation 'hotspots', we favor an explanation based on
425 strong selection on gene function, with region-specific mutation rates playing, at best, a secondary
426 role in *A. thaliana* mitogenomes.
427
428 **Uneven copy number across angiosperm mitogenomes and implications for models of**
429 **genome structure.**
430 Our analysis of a published sequencing dataset from MA lines (JIANG *et al.* 2014) and newly
431 sequenced samples of purified mtDNA found evidence that coverage across the mitogenome is not
432 constant and that it can show detectable levels of divergence across MA lines. Patterns of coverage
433 variation were largely continuous (Figures 1 and 3), which contrasts with other commonly studied
434 forms of copy number variation, in which germ-line segmental duplications or losses result in
435 discrete shifts in coverage for specific regions of the genome (CONRAD *et al.* 2010). Our findings are
436 relevant to previous work in the mitogenome of *Mimulus guttatus*, in which alternative recombination-
437 mediated conformations showed evidence of heterogenous coverage, even in some cases where
438 they were predicted to be part of the same subgenomic molecules (MOWER *et al.* 2012a). In addition,
439 it has been shown that, disruption of specific nuclear genes involved in mitogenome replication,
440 recombination, and repair can lead to preferential amplification or loss of certain genomic regions
441 (SHEDGE *et al.* 2007; WALLET *et al.* 2015), and recent evidence indicates that mitogenome copy
442 number can change in gene-specific ways across development in *Cucumis melo* (SHEN et al. 2019).
443 Other analyses of intraspecific mitogenome variation in systems such as *A. thaliana* (DAVILA
444 et al. 2011), *Beta vulgaris* (DARRACQ *et al.* 2011), and *Zea mays* (ALLEN *et al.* 2007; DARRACQ *et al.*
445 2010) have generally focused on structural rearrangements resulting from repeat-mediated
446 recombination. Indeed, at an even finer level, angiosperm mitogenomes are really a population of
447 alternative structures that interconvert via recombination and coexist within cells and tissues in a
448 single individual (PALMER and SHIELDS 1984; GUALBERTO and NEWTON 2017; KOZIK *et al.* 2019). As
449 such, these structural rearrangements are arguably the most dynamic element of plant mtDNA

450 evolution, and rapid shifts in the predominant structure (referred to as substoichiometric shifting) are
451 often observed on very short generational timescales (ABDELNOOR *et al.* 2003; ARRIETA-MONTIEL and
452 MACKENZIE 2011). However, when it comes to the MA-line analysis in this study, it is notable that it
453 was copy number variation and not structural rearrangements for which we could detect significant
454 divergence among lines. Therefore, in this case, it appears that copy number variation might be the
455 most rapidly diverging feature of the *A. thaliana* mitogenome, even though the general pattern of
456 coverage is quite similar across lines (Figure 1) and there is known to be a persistent level of
457 recombinational activity that is constantly occurring and interconverting amongst the population of
458 alternative mitogenome structures. The divergence in copy number among lines did not appear to be
459 entirely random, as we detected significant differences associated with salt-stress treatments,
460 suggesting that the historical environment experienced in recent generations can have an effect in
461 shaping the mitogenome landscape.
462 When identifying copy number variation among lines, it is important to consider a number of
463 alternative explanations. As described above, we investigated the possibility that PCR or sequencing
464 bias associated with nucleotide composition could explain variation in coverage but found very little
465 explanatory power from such effects. Another possibility is that differences among lines represent
466 heterogeneous sampling, such as different developmental timepoints, as there is evidence of locus-
467 specific mitochondrial copy number variation across development (SHEN et al. 2019). Such
468 differences may contribute to the contrasting patterns of variation between the MA lines of Jiang et
469 al. (2014) and our purified mtDNA samples (Figures 1, 3, and S4), as these were grown and
470 sampled at different times and in different labs. It is less likely that developmental differences explain
471 observed divergence between salt-stressed and control MA lines because these were all grown and
472 sampled under common garden conditions in the final generation of the experiment. Nevertheless,
473 we cannot rule out the possibility that lines from different treatments exhibited systematic differences
474 in growth such that sampling in the original MA study effectively represented different developmental
475 stages.
476 A further assumption made in analyzing copy number variation is that DNA extraction
477 methods representatively sample the entire genome. Although this is likely to be a reasonable
478 assumption in most cases, it is plausible that procedures that rely on mitochondrial isolation may
479 differentially enrich for certain subpopulations of mitochondria that may differ in their genomic
480 content. The low ratio of mitochondrial genome copies to actual mitochondrial organelles in
481 *Arabidopsis* tissues implies that many mitochondria harbor only partial mitochondrial genomes or no
482 mtDNA at all (PREUTEN et al. 2010). This and other characteristics of our mtDNA isolation protocol
483 (e.g., storage in the dark prior to isolation or use of DNase to remove contaminating nuclear and
484 plastid DNA) may be an additional cause of the contrasting patterns between the MA lines and our
485 purified mtDNA samples. It might also explain why ddPCR found smaller differences between high-

486 copy and low-copy markers in total-cellular DNA than in purified mtDNA samples (Figure 4).
487 However, the observed difference between total-cellular DNA and purified mtDNA may also simply
488 reflect another example of regression to the mean, as ddPCR was performed on the exact sample
489 purified mtDNA samples that were sequenced and used to define high-copy and low-copy markers,
490 while the total-cellular sample was an independent extraction from different tissue. Once again, the
491 effects of different DNA extraction methods are unlikely to explain divergence between MA lines
492 because they were all processed with the same total-cellular method (JIANG *et al.* 2014).
493 Angiosperm mitogenome sequencing projects typically report genome assemblies
494 represented as a single circular structure, but it is widely accepted that this is an oversimplification
495 resulting from mapping and that the physical form of angiosperm mtDNA involves complex
496 branching structures (BENDICH 1993; SLOAN 2013; KOZIK *et al.* 2019). These branching structures
497 likely reflect the activity of DNA replication, which is thought to be initiated by recombination-
498 dependent mechanisms and not depend on a single origin of replication (CUPP and NIELSEN 2014).
499 In addition to findings from more direct observations of the physical form of mtDNA molecules
500 (BENDICH 1996; BACKERT and BORNER 2000), coverage patterns in previous sequencing efforts have
501 been interpreted as evidence against a 'master circle' as the predominant form of the mitogenome
502 (MOWER *et al.* 2012a).
503 By itself, copy number variation is not definitive evidence against a simple circular
504 organization in *A. thaliana.* Bacterial genomes are circular structures but can still exhibit quantitative
505 variation in coverage across the genome when DNA is sampled from actively dividing cultures, with
506 copy number decreasing from the origin of replication to the terminus of replication. Indeed,
507 analyzing sequencing coverage of bacterial genomes can be an effective way to identify the location
508 of the origin of replication and measure the replication rate of bacteria (BROWN *et al.* 2016). In
509 addition, it is possible that variation in coverage could reflect differential degradation, either occurring
510 naturally over the course of development (KUMAR et al 2014) or as an artefact of the extraction
511 process. Nevertheless, we contend that the combination of heterogeneous coverage and evidence
512 for shifts in copy number variation among MA lines is unlikely to be explained by a simple circular
513 model with preferential amplification at origin(s) of replication or differential degradation within the
514 circle, especially when viewed in the light of existing evidence against the master circle as a
515 predominant genome form. Instead, our results suggest that the complex physical structure of
516 angiosperm mitogenomes creates opportunities for differential amplification or degradation of
517 subgenomic regions in a dynamic way that does not occur in simpler mitogenomes like those found
518 in bilaterian animals. In addition to the rapid and large changes in the frequencies of mitogenome
519 structural conformations associated with substoichiometric shifting, angiosperms appear to be
520 subject to more pervasive low-level fluctuations in copy numbers of local regions within the genome.
521

522

523 **ACKNOWLEDGEMENTS**

524

525 We thank Jeff Mower for helpful discussion and motivation to use intraspecific variation to analyze
526 contrasting patterns of evolution between genic and intergenic regions in plant mitogenomes. We
527 also thank the Associate Editor and an anonymous reviewer for their insightful comments on an
528 earlier version of this manuscript. This work was supported by a grant from the NIH (R01
529 GM118046) and an NSF NRT GAUSSI Graduate Fellowship (DGE-1450032).

REFERENCES

Abdelnoor, R. V., R. Yule, A. Elo, A. C. Christensen, G. Meyer-Gauen *et al.*, 2003 Substoichiometric shifting in the plant mitochondrial genome is influenced by a gene homologous to MutS. Proceedings of the National Academy of Sciences 100**:** 5968-5973.

Aird, D., M. G. Ross, W. S. Chen, M. Danielsson, T. Fennell *et al.*, 2011 Analyzing and minimizing PCR amplification bias in Illumina sequencing libraries. Genome biology 12**:** R18.

Allen, J. O., C. M. Fauron, P. Minx, L. Roark, S. Oddiraju *et al.*, 2007 Comparisons among two fertile and three male-sterile mitochondrial genomes of maize. Genetics 177**:** 1173-1192.

Alonso-Blanco, C., J. Andrade, C. Becker, F. Bemm, J. Bergelson *et al.*, 2016 1,135 genomes reveal the global pattern of polymorphism in *Arabidopsis thaliana*. Cell 166**:** 481-491.

Arrieta-Montiel, M. P., and S. A. Mackenzie, 2011 Plant mitochondrial genomes and recombination, pp. 65-82 in *Plant Mitochondria*, edited by F. Kempken. Springer Verlag, New York.

Arrieta-Montiel, M. P., V. Shedge, J. Davila, A. C. Christensen and S. A. Mackenzie, 2009 Diversity of the Arabidopsis mitochondrial genome occurs via nuclear-controlled recombination activity. Genetics 183**:** 1261-1268.

Backert, S., and T. Borner, 2000 Phage T4-like intermediates of DNA replication and recombination in the mitochondria of the higher plant Chenopodium album (L.). Current genetics 37**:** 304-314.

Bendich, A. J., 1993 Reaching for the ring: the study of mitochondrial genome structure. Current genetics 24**:** 279-290.

Bendich, A. J., 1996 Structural analysis of mitochondrial DNA molecules from fungi and plants using moving pictures and pulsed-field gel electrophoresis. Journal of Molecular Biology 255**:** 564-588.

Benjamini, Y., and Y. Hochberg, 1995 Controlling the False Discovery Rate: A Practical and Powerful Approach to Multiple Testing. Journal of the Royal Statistical Society.Series B (Methodological) 57**:** 289-300.

Brown, C. T., M. R. Olm, B. C. Thomas and J. F. Banfield, 2016 Measurement of bacterial replication rates in microbial communities. Nature Biotechnology 34**:** 1256-1263.

Brown, W. M., M. George and A. C. Wilson, 1979 Rapid evolution of animal mitochondrial DNA. Proceedings of the National Academy of Sciences 76**:** 1967-1971.

Chamary, J. V., J. L. Parmley and L. D. Hurst, 2006 Hearing silence: non-neutral evolution at synonymous sites in mammals. Nature reviews.Genetics 7**:** 98-108.

Christensen, A. C., 2013 Plant mitochondrial genome evolution can be explained by DNA repair mechanisms. Genome Biology and Evolution 5**:** 1079-1086.

Christensen, A. C., 2014 Genes and junk in plant mitochondria-repair mechanisms and selection. Genome Biology and Evolution 6**:** 1448-1453.

Conrad, D. F., D. Pinto, R. Redon, L. Feuk, O. Gokcumen *et al.*, 2010 Origins and functional impact of copy number variation in the human genome. Nature 464**:** 704-712.
Cupp, J. D., and B. L. Nielsen, 2014 DNA replication in plant mitochondria. Mitochondrion 19**:** 231-237.
Darracq, A., J. S. Varre, L. Marechal-Drouard, A. Courseaux, V. Castric *et al.*, 2011 Structural and content diversity of mitochondrial genome in beet: a comparative genomic analysis. Genome biology and evolution 3**:** 723-736.
Darracq, A., J. S. Varre and P. Touzet, 2010 A scenario of mitochondrial genome evolution in maize based on rearrangement events. BMC genomics 11**:** 233.
Davila, J. I., M. P. Arrieta-Montiel, Y. Wamboldt, J. Cao, J. Hagmann *et al.*, 2011 Double-strand break repair processes drive evolution of the mitochondrial genome in Arabidopsis. BMC biology 9**:** 64.
Doyle, J. J., and J. L. Doyle, 1987 A rapid DNA isolation procedure for small quantities of fresh leaf tissue. Phytochemical bulletin 19**:** 11-15.
Drouin, G., H. Daoud and J. Xia, 2008 Relative rates of synonymous substitutions in the mitochondrial, chloroplast and nuclear genomes of seed plants. Molecular Phylogenetics and Evolution 49**:** 827-831.
Ellis, J., 1982 Promiscuous DNA--chloroplast genes inside plant mitochondria. Nature 299**:** 678-679.
Goremykin, V. V., P. J. Lockhart, R. Viola and R. Velasco, 2012 The mitochondrial genome of Malus domestica and the import-driven hypothesis of mitochondrial genome expansion in seed plants. The Plant Journal 71**:** 615-626.
Gualberto, J. M., and K. J. Newton, 2017 Plant mitochondrial genomes: dynamics and mechanisms of mutation. Annual Review of Plant Biology 68**:** 225-252.
Halligan, D. L., and P. D. Keightley, 2009 Spontaneous mutation accumulation studies in evolutionary genetics. Annual Review of Ecology, Evolution, and Systematics 40**:** 151-172.
Hanawalt, P. C., and G. Spivak, 2008 Transcription-coupled DNA repair: two decades of progress and surprises. Nature Reviews Molecular Cell Biology 9**:** 958-970.
Harris, K., and R. Nielsen, 2014 Error-prone polymerase activity causes multinucleotide mutations in humans. Genome Research 24**:** 1445-1454.
Hazkani-Covo, E., R. M. Zeller and W. Martin, 2010 Molecular poltergeists: mitochondrial DNA copies (numts) in sequenced nuclear genomes. PLoS Genetics 6**:** e1000834.
Jiang, C., A. Mithani, E. J. Belfield, R. Mott, L. D. Hurst *et al.*, 2014 Environmentally responsive genome-wide accumulation of de novo Arabidopsis thaliana mutations and epimutations. Genome Research 24**:** 1821-1829.
Kozik, A., B. Rowan, D. Lavelle, L. Berke, M. E. Schranz *et al.*, 2019 The alternative reality of plant mitochondrial DNA: One ring does not rule them all. PLoS Genetics**:** e1008373.
Kubo, T., and K. J. Newton, 2008 Angiosperm mitochondrial genomes and mutations. Mitochondrion 8**:** 5-14.
Kumar, R. A., D. J. Oldenburg and A. J. Bendich, 2014 Changes in DNA damage, molecular integrity, and copy number for plastid DNA and mitochondrial DNA during maize development. Journal of Experimental Botany 65: 6425-6439.
Langmead, B., and S. L. Salzberg, 2012 Fast gapped-read alignment with Bowtie 2. Nature Methods 9**:** 357-359.
Li, H., B. Handsaker, A. Wysoker, T. Fennell, J. Ruan *et al.*, 2009 The Sequence Alignment/Map format and SAMtools. Bioinformatics (Oxford, England) 25**:** 2078-2079.
Lonsdale, D. M., T. Brears, T. P. Hodge, S. E. Melville and W. H. Rottmann, 1988 The plant mitochondrial genome: homologous recombination as a mechanism for generating heterogeneity. Philosophical Transactions of the Royal Society of London.B, Biological Sciences 319**:** 149-163.
Martin, M., 2011 Cutadapt removes adapter sequences from high-throughput sequencing reads. EMBnet.journal 17**:** 10-12.

McKenna, A., M. Hanna, E. Banks, A. Sivachenko, K. Cibulskis *et al.*, 2010 The Genome Analysis Toolkit: a MapReduce framework for analyzing next-generation DNA sequencing data. Genome Research 20**:** 1297-1303.

Mower, J. P., A. L. Case, E. R. Floro and J. H. Willis, 2012a Evidence against equimolarity of large repeat arrangements and a predominant master circle structure of the mitochondrial genome from a monkeyflower (Mimulus guttatus) lineage with cryptic CMS. Genome Biology and Evolution 4**:** 670-686.

Mower, J. P., D. B. Sloan and A. J. Alverson, 2012b Plant mitochondrial diversity – the genomics revolution, pp. 123-144 in *Plant Genome Diversity*, edited by J. F. Wendel. Springer, Vienna.

Nielsen, R., 2005 Molecular signatures of natural selection. Annual Review of Genetics 39**:** 197-218.

Palmer, J. D., and C. R. Shields, 1984 Tripartite structure of the Brassica campestris mitochondrial genome. Nature 307**:** 437-440.

Preuten, T., E. Cincu, J. Fuchs, R. Zoschke, K. Liere, T. Börner, 2010 Fewer genes than organelles: extremely low and variable gene copy numbers in mitochondria of somatic plant cells. Plant Journal. 64: 948-959.

Rice, D. W., A. J. Alverson, A. O. Richardson, G. J. Young, M. V. Sanchez-Puerta *et al.*, 2013 Horizontal transfer of entire genomes via mitochondrial fusion in the angiosperm Amborella. Science 342**:** 1468-1473.

Robinson, J. T., H. Thorvaldsdóttir, A. M. Wenger, A. Zehir and J. P. Mesirov, 2017 Variant review with the integrative genomics viewer. Cancer Research 77**:** e31-e34.

Schrider, D. R., J. N. Hourmozdi and M. W. Hahn, 2011 Pervasive multinucleotide mutational events in eukaryotes. Current Biology 21**:** 1051-1054.

Shedge, V., M. Arrieta-Montiel, A. C. Christensen and S. A. Mackenzie, 2007 Plant mitochondrial recombination surveillance requires unusual RecA and MutS homologs. The Plant Cell 19**:** 1251-1264.

Shen, J., Y. Zhang, M. J. Havey and W. Shou, 2019 Copy numbers of mitochondrial genes change during melon leaf development and are lower than the numbers of mitochondria. Horticulture Research 6**:** 95.

Sloan, D. B., 2013 One ring to rule them all? Genome sequencing provides new insights into the 'master circle' model of plant mitochondrial DNA structure. New Phytologist 200**:** 978-985.

Sloan, D. B., J. C. Havird and J. Sharbrough, 2017 The on-again, off-again relationship between mitochondrial genomes and species boundaries. Molecular Ecology 26**:** 2212-2236.

Sloan, D. B., K. Muller, D. E. McCauley, D. R. Taylor and H. Storchova, 2012 Intraspecific variation in mitochondrial genome sequence, structure, and gene content in Silene vulgaris, an angiosperm with pervasive cytoplasmic male sterility. The New Phytologist 196**:** 1228-1239.

Sloan, D. B., and D. R. Taylor, 2010 Testing for selection on synonymous sites in plant mitochondrial DNA: the role of codon bias and RNA editing. Journal of Molecular Evolution 70**:** 479-491.

Sloan, D. B., and Z. Wu, 2014 History of plastid DNA insertions reveals weak deletion and at mutation biases in angiosperm mitochondrial genomes. Genome Biology and Evolution 6**:** 3210-3221.

Sloan, D. B., Z. Wu and J. Sharbrough, 2018 Correction of persistent errors in Arabidopsis reference mitochondrial genomes. Plant Cell 30**:** 525-527.

Small, I. D., P. G. Isaac and C. J. Leaver, 1987 Stoichiometric differences in DNA molecules containing the atpA gene suggest mechanisms for the generation of mitochondrial genome diversity in maize. The EMBO journal 6**:** 865-869.

Stajich, J. E., D. Block, K. Boulez, S. E. Brenner, S. A. Chervitz *et al.*, 2002 The Bioperl toolkit: Perl modules for the life sciences. Genome research 12**:** 1611-1618.

Stupar, R. M., J. W. Lilly, C. D. Town, Z. Cheng, S. Kaul *et al.*, 2001 Complex mtDNA constitutes an approximate 620-kb insertion on Arabidopsis thaliana chromosome 2: implication of potential sequencing errors caused by large-unit repeats. Proceedings of the National Academy of Sciences of the United States of America 98**:** 5099-5103.

van Dijk, E. L., Y. Jaszczyszyn and C. Thermes, 2014 Library preparation methods for next-generation sequencing: tone down the bias. Experimental Cell Research 322**:** 12-20.

Venkat, A., M. W. Hahn and J. W. Thornton, 2018 Multinucleotide mutations cause false inferences of lineage-specific positive selection. Nature Ecology & Evolution 2**:** 1280-1288.

Wallet, C., M. Le Ret, M. Bergdoll, M. Bichara, A. Dietrich *et al.*, 2015 The RECG1 DNA translocase is a key factor in recombination surveillance, repair, and segregation of the mitochondrial DNA in Arabidopsis. Plant Cell 27**:** 2907-2925.

Warren, J. M., M. P. Simmons, Z. Wu and D. B. Sloan, 2016 Linear plasmids and the rate of sequence evolution in plant mitochondrial genomes. Genome Biology and Evolution 8**:** 364-374.

Wolfe, K. H., W. H. Li and P. M. Sharp, 1987 Rates of nucleotide substitution vary greatly among plant mitochondrial, chloroplast, and nuclear DNAs. Proceedings of the National Academy of Sciences of the United States of America 84**:** 9054-9058.

Wynn, E. L., and A. C. Christensen, 2015 Are synonymous substitutions in flowering plant mitochondria neutral? Journal of Molecular Evolution 81**:** 131-135.

Yang, Z., and A. D. Yoder, 1999 Estimation of the transition/transversion rate bias and species sampling. Journal of Molecular Evolution 48**:** 274-283.

Zhu, A., W. Guo, K. Jain and J. P. Mower, 2014 Unprecedented heterogeneity in the synonymous substitution rate within a plant genome. Molecular Biology and Evolution 31**:** 1228-1236.

Table 1. Variant statistics for 1001 Genomes dataset. SNPs: single nucleotide polymorphisms; MAF: minor allele frequency.

Sequence Type	Sites	SNPs	SNPs per Site	SNP MAF	Indels	Indels per Site	Indel MAF
Protein Coding	31264	41	0.0013	0.0206	0	0.0000	NA
Nonsynonymous	24323	22	0.0009	0.0244	0	0.0000	NA
Synonymous	6941	19	0.0027	0.0163	0	0.0000	NA
rRNA	5222	3	0.0006	0.0010	0	0.0000	NA
tRNA	1689	0	0.0000	NA	0	0.0000	NA
Pseudogene	1256	5	0.0040	0.0025	0	0.0000	NA
Intron	35335	72	0.0020	0.0218	18	0.0005	0.0116
Intergenic	293042	987	0.0034	0.0263	172	0.0006	0.0239
Total	**367808**	**1108**	**0.0030**	**0.0256**	**190**	**0.0005**	**0.0006**

Figure 1. Sequencing coverage variation across mitogenome of *Arabidopsis thaliana* mutation accumulation lines. Each panel represents an average of three biological replicates. Red vertical lines at the bottom of the figure represent the two pairs of large, identical repeats in the *A. thaliana* mitogenome. When each Illumina read is mapped to these repeats, bowtie2 randomly assigns the read to one copy, so coverage estimates are not expected to be elevated in these regions. The blue dashed line indicates mean coverage for the sample.

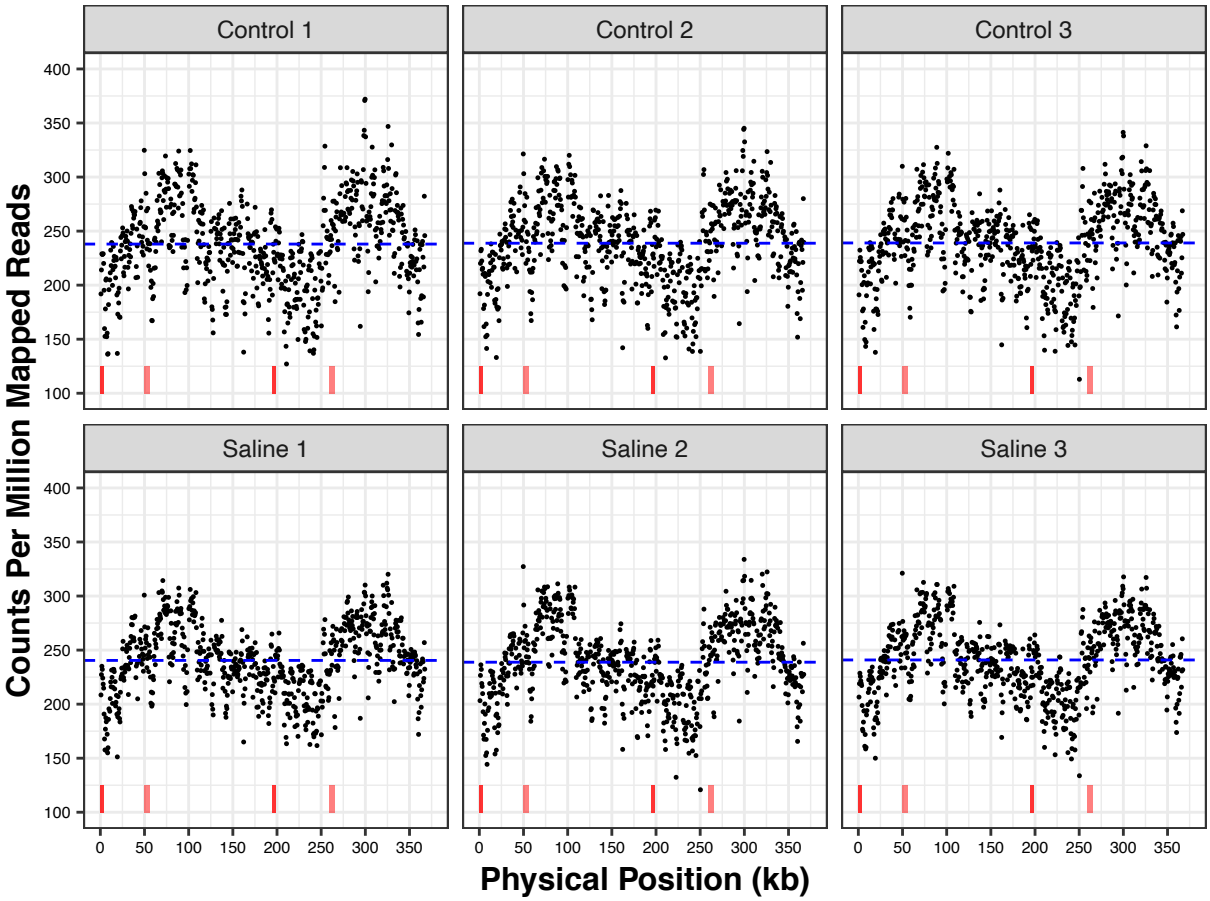

Figure 2. Divergence in region-specific mitogenome copy number in salt-stressed vs. control mutation accumulation lines. Values are expressed as a ratio of the averages for all salt-stressed and all control lines. Windows that deviate significantly from a ratio of 1 after false-discovery-rate correction are highlighted in red. CPMM: counts per million mapped reads.

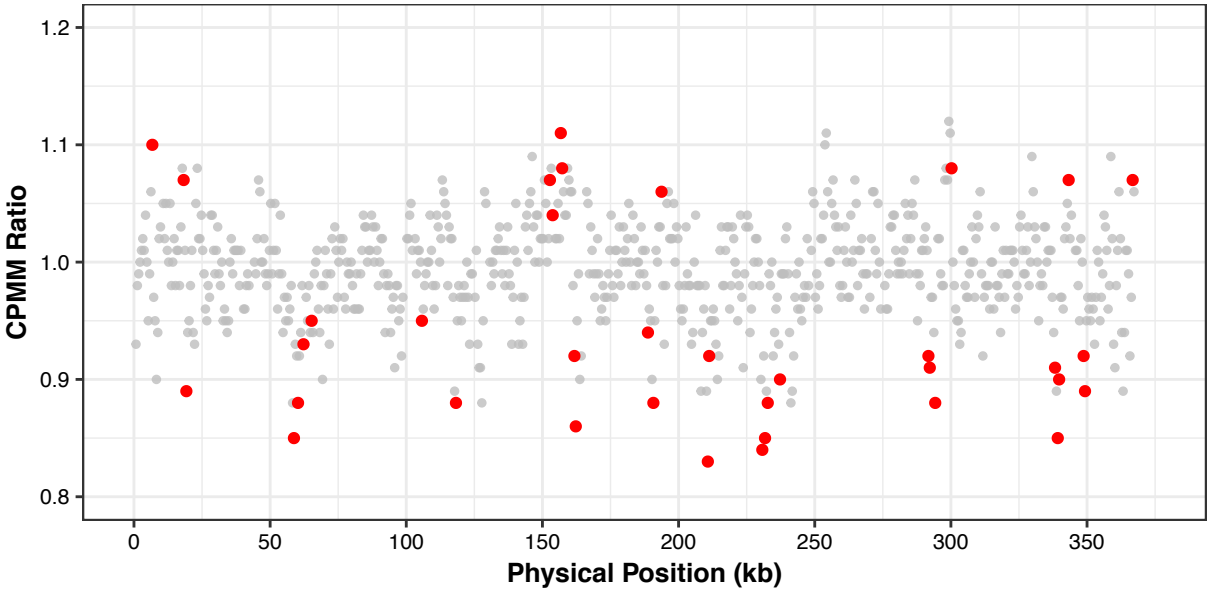

Figure 3. Sequencing coverage variation across the mitogenome for three purified mtDNA samples from *Arabidopsis thaliana*. The windows chosen for development of ddPCR markers are shown in red and blue dots (high- and low-coverage regions, respectively). Red vertical lines at the bottom of the figure represent the two pairs of large, identical repeats in the *A. thaliana* mitogenome. When each Illumina read is mapped to these repeats, bowtie2 randomly assigns the read to one copy, so coverage estimates are not expected to be elevated in these regions. The blue dashed line indicates mean coverage for the sample.

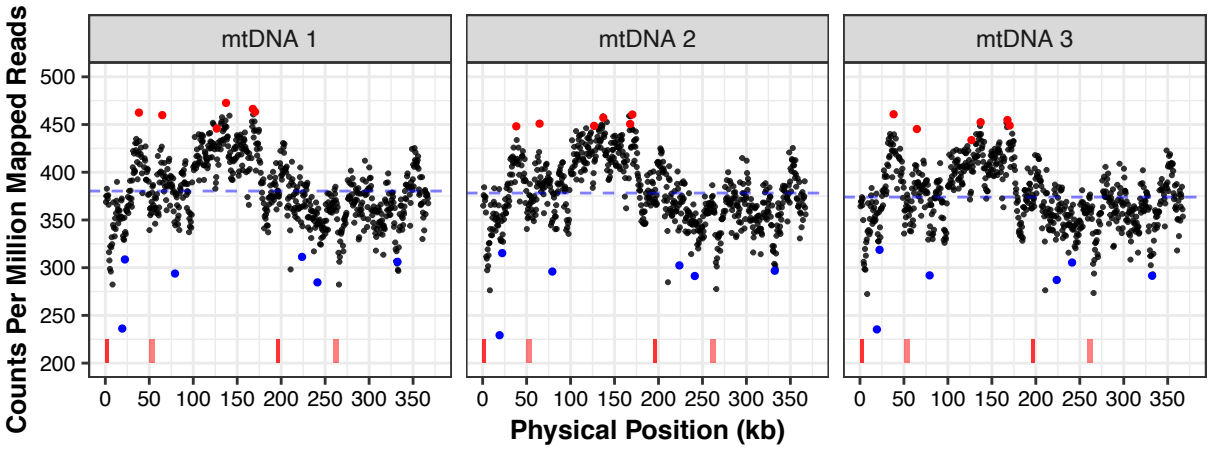

Figure 4. ddPCR comparison of copy number for mitogenome regions identified as either high-copy or low-copy by sequencing analysis. Copy numbers are expressed as per μl of ddPCR reaction volume. Input for the mtDNA samples was diluted 200-fold relative to the total-cellular sample.